Acta Mechanica Sinica (2019) 35(2):338–342
https://doi.org/10.1007/s10409-019-00850-5

RESEARCH PAPER

Volumetric response of an ellipsoidal liquid inclusion: implications for cell mechanobiology

Xin Chen[1,2,3] · Wei He[1,2] · Shaobao Liu[3,4] · Moxiao Li[1,2] · Guy M. Genin[2,4,5] · Feng Xu[2,4] · Tian Jian Lu[3,6]

Received: 12 December 2018 / Revised: 18 January 2019 / Accepted: 24 January 2019 / Published online: 4 April 2019

Abstract
Elastic composites containing liquid inclusions exist widely in nature and in engineered systems. The volumetric response of liquid inclusions is important in many cases, such as an isolated cell embedded in an extracellular matrix or an oil pocket embedded within shale. In this study, we developed a model for describing the volumetric response of an ellipsoidal liquid inclusion. Specifically, we investigated the volumetric response of an ellipsoidal liquid inclusion embedded in a three-dimensional (3D) matrix through an analytical expression of the volumetric response. We performed parametric analysis and found that loading along the shortest axis can induce the most volume change, while loading along the longest axis can induce the least volume change. We also found that the volumetric response decreases with increasing Poisson ratio of the matrix. These results could be used to understand some cell behavior in a 3D matrix, for example, cell alignment under mechanical load.

Keywords Liquid inclusion · Liquid compressibility · Inclusion theory · Solid–liquid interaction

✉ Feng Xu
fengxu@mail.xjtu.edu.cn

✉ Tian Jian Lu
tjlu@mail.xjtu.edu.cn

Wei He
a19931230@stu.xjtu.edu.cn

1 State Key Laboratory for Strength and Vibration of Mechanical Structures, Xi'an Jiaotong University, Xi'an 710049, China

2 Bioinspired Engineering and Biomechanics Center (BEBC), Xi'an Jiaotong University, Xi'an 710049, China

3 State Key Laboratory of Mechanics and Control of Mechanical Structures, Nanjing University of Aeronautics and Astronautics, Nanjing 210016, China

4 Key Laboratory of Biomedical Information Engineering of Ministry of Education, Xi'an Jiaotong University, Xi'an 710049, China

5 U.S. National Science Foundation Science and Technology Center for Engineering Mechanobiology, Washington University, St. Louis, MO 63130, USA

6 Nanjing Center for Multifunctional Lightweight Materials and Structures (MLMS), Nanjing University of Aeronautics and Astronautics, Nanjing 210016, China

1 Introduction

Liquid inclusions in a three-dimensional (3D) matrix exist widely in nature and in engineered systems, such as in rocks [1], soft composites [2, 3], actuators [4], polymer dispersed liquid crystal systems [5], and, under certain conditions, in biological tissues [6]. In these examples, liquid inclusions are often under mechanical load and their volumetric response is important. For instance, the volume response of an oil and gas pocket embedded in shale is related to oil production. The volumetric response of cells embedded in an extracellular matrix (ECM) could play an important role in their physiological behaviors [7].

Work in both two-dimensional (2D) and 3D has shown that cells fluidize in response to high levels of mechanical stretch [8–10]. Over time, cells can rearrange in a way that depends on their mechanical microenvironment, which, in 3D, typically leads to cell realignment in the direction of greatest mechanical stretch [11–16]. A key feature of this in 3D is that they additionally change their mechanical microenvironment [17]. This remodeling of both cells and ECM leads to a matching of cell and ECM stiffness [18]. The models that underlie these interpretations typically treat cells as solids [19]. However, transitions in shape might occur most effectively under cyclical loading, as cells best fluidize under these conditions [15]. We therefore explored whether the volumetric response of a liquid inclusion might vary with the direction of loading in a way that is predictive of cell realignment to mechanical stretch in 3D.

Although efforts have been undertaken to understand the behaviors of liquid inclusions via experiment [20, 21] and simulation [22], these approaches are incapable of providing detailed information about the volume response of liquid inclusions. To address this, two approaches have been developed to deal with liquid inclusions. On one hand, based on Eshelby's work [23] for solid inclusions, Shafiro and Kachanov [24] and Chen et al. [25] derived the elastic fields of single liquid inclusion embedded within a 3D matrix. These studies, however, did not give detailed analysis of the volumetric response of the liquid inclusion. On the other hand, by stress potential functions, Mancarella et al. [26] and Style et al. [27] gave an explicit expression to describe the inclusion behaviors. However, their model assumed the liquid to be incompressible, which may not be true, especially for cells.

In this study, we performed a detailed analysis of the volumetric response of an ellipsoidal compressible liquid inclusion embedded within an infinite elastic matrix under mechanical loading. We first describe the problem and give the volume response of the liquid inclusion by Eshelby's method [23, 28]. We decompose our results to give explicit solutions for spherical and spheroidal inclusions. We investigate how the inclusion shape, loading type and matrix Poisson ratio influence the inclusion volume response. Finally, as a demonstration, we relate our results with some phenomena in cell mechanics.

2 Problem statement and solution

Firstly, we consider an ellipsoidal liquid inclusion imbedded in an infinite and linear elastic matrix (Fig. 1). The semi-axes of the inclusion in the x_1, x_2, and x_3 directions are of lengths a_1, a_2, and a_3 ($a_1 \geq a_2 \geq a_3$) (Fig. 1). We assume that the initial pressure of the liquid is zero, so that the matrix is free of stress before far field loading is applied. We further assume that the liquid inclusion is sufficiently large so that surface effects at the liquid-matrix interface may be neglected. Upon loading, according to linear elasticity, the governing equations in the matrix are given as

$$\begin{aligned} \boldsymbol{\varepsilon} &= \frac{1}{2}(\nabla \boldsymbol{u} + \boldsymbol{u}\nabla), \\ \boldsymbol{\sigma} &= \frac{E}{1+\nu}\left[\frac{\nu}{1-2\nu}\mathrm{tr}(\boldsymbol{\varepsilon}) + \boldsymbol{\varepsilon}\right], \\ \nabla \cdot \boldsymbol{\sigma} &= 0, \end{aligned} \tag{1}$$

where $\boldsymbol{u}$, $\boldsymbol{\varepsilon}$, and $\boldsymbol{\sigma}$ are the displacement vector field, strain tensor field, and stress tensor field in the matrix, respectively, and E (N/m^2) and ν are Young's modulus and Poisson ratio of the matrix material.

Let the liquid be linearly compressible, namely

$$k\frac{\Delta V}{V} = -p, \tag{2}$$

where k (N/m^2) is the bulk modulus of the liquid, V and ΔV are the initial volume and volume change of the inclusion, respectively, and p is the liquid pressure after loading.

We define $\boldsymbol{\varepsilon}^\infty$ as the constant far field matrix strain tensor (Fig. 1). At the interface between the inclusion and the matrix, the stress of the matrix is balanced by the liquid pressure as

$$\boldsymbol{\sigma} \cdot \boldsymbol{n} = -p\boldsymbol{n}, \tag{3}$$

where $\boldsymbol{n}$ is the unit outer normal vector of the interface. According to our previous work [25], the volume change induced by the far field load can be expressed by

$$\frac{\Delta V}{V} = \mathrm{tr}\left\{\left[\boldsymbol{I} + \boldsymbol{S} : \boldsymbol{L}_0^{-1} : \left(\boldsymbol{L}_1 - \boldsymbol{L}_0\right)\right]^{-1} : \boldsymbol{\varepsilon}^\infty\right\}, \tag{4}$$

where tr(·) is the trace of the second-order tensor, and the fourth-rank tensors $\boldsymbol{L}_1$ and $\boldsymbol{L}_0$ are the "stiffness tensors" of the liquid and matrix, respectively

$$\begin{aligned} \left(\boldsymbol{L}_0\right)_{ijkl} &= \frac{E\nu}{(1+\nu)(1-2\nu)}\delta_{ij}\delta_{kl} + \frac{E}{1+\nu}\delta_{ik}\delta_{jl}, \\ \left(\boldsymbol{L}_1\right)_{ijkl} &= k\delta_{ij}\delta_{kl}. \end{aligned} \tag{5}$$

$\boldsymbol{S}$ is the Eshelby tensor for the ellipsoidal inclusion, whose components can be expressed as

$$\begin{aligned} S_{iiii} &= \frac{3}{8\pi(1-\nu)}a_i^2 I_{ii} + \frac{1-2\nu}{8\pi(1-\nu)}I_i, \\ S_{iijj} &= \frac{3}{8\pi(1-\nu)}a_j^2 I_{ij} - \frac{1-2\nu}{8\pi(1-\nu)}I_i, \\ S_{ijij} &= \frac{a_1^2 + a_2^2}{16\pi(1-\nu)}I_{ij} + \frac{1-2\nu}{16\pi(1-\nu)}\left(I_i + I_j\right), \\ & i,j = 1,2,3,\ i \neq j, \end{aligned} \tag{6}$$

in which the elliptical integrals are

$$\begin{aligned} I_i &= 2\pi a_1 a_2 a_3 \int_0^\infty \frac{\mathrm{d}s}{\left(a_i^2 + s\right)\Delta s}, \\ I_{ii} &= 2\pi a_1 a_2 a_3 \int_0^\infty \frac{\mathrm{d}s}{\left(a_i^2 + s\right)^2 \Delta s}, \\ I_{ij} &= 2\pi a_1 a_2 a_3 \int_0^\infty \frac{\mathrm{d}s}{\left(a_i^2 + s\right)\left(a_j^2 + s\right)\Delta s}, \end{aligned} \tag{7}$$

$i,j = 1, 2, 3$ and $i \neq j$.

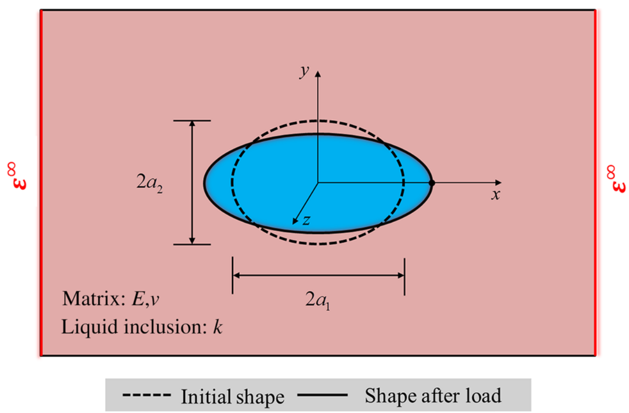

Fig. 1 Schematic of the problem. An ellipsoidal, compressible liquid inclusion embedded within a linear-elastic solid matrix subjected to far field load. The axial lengths of the inclusion are a_1, a_2, and a_3 ($a_1 \geq a_2 \geq a_3$, where a_3 is the axial length of the z direction and is not marked in the figure). The x, y, and z directions of the Cartesian system are parallel with the axes of a_1, a_2, and a_3, respectively

For special cases including spherical and spheroidal inclusions, these integrals can be simplified as explicit expressions as follows

Case 1 Sphere ($a_1 = a_2 = a_3 = a$)

$$I_1 = I_2 = I_3 = \frac{4\pi}{3},$$
$$I_{11} = I_{22} = I_{33} = I_{12} = I_{23} = I_{31} = \frac{4\pi}{5a^2}. \tag{8}$$

Case 2 Oblate spheroid ($a_1 = a_2 > a_3$)

$$I_1 = I_2 = \frac{2\pi a_1^2 a_3}{\left(a_1^2 - a_3^2\right)^{3/2}}\left[\arccos\left(\frac{a_3}{a_1}\right) - \frac{a_3}{a_1}\left(1 - \frac{a_3^2}{a_1^2}\right)^{1/2}\right],$$
$$I_3 = 4\pi - 2I_1, I_{11} = I_{22} = I_{12} = \frac{\pi}{a_1^2} - \frac{I_1 - I_3}{4\left(a_3^2 - a_1^2\right)},$$
$$I_{13} = I_{23} = \frac{I_1 - I_3}{a_3^2 - a_1^2}, I_{33} = \frac{1}{3}\left(\frac{4\pi}{a_3^2} - 2I_{13}\right).$$
$$I_{11} = I_{22} = I_{33} = I_{12} = I_{23} = I_{31} = \frac{4\pi}{5a^2}. \tag{9}$$

Case 3 Prolate spheroid ($a_1 > a_2 = a_3$)

$$I_2 = I_3 = \frac{2\pi a_1 a_3^2}{\left(a_1^2 - a_3^2\right)^{3/2}}\left[\frac{a_1}{a_3}\left(\frac{a_1^2}{a_3^2} - 1\right)^{1/2} - \cosh^{-1}\left(\frac{a_1}{a_3}\right)\right],$$
$$I_3 = 4\pi - 2I_2, I_{22} = I_{33} = I_{23} = \frac{\pi}{a_2^2} - \frac{I_2 - I_1}{4\left(a_1^2 - a_2^2\right)},$$
$$I_{13} = I_{12} = \frac{I_2 - I_1}{a_1^2 - a_2^2}, I_{11} = \frac{1}{3}\left(\frac{4\pi}{a_1^2} - 2I_{12}\right). \tag{10}$$

3 Results

1. Shear does not affect the volume of an inclusion.

First, we note that the components of $\boldsymbol{S}$ are zero except for S_{iijj} and S_{ijij} $(i, j = 1, 2, 3)$. According to Eqs. (4) and (5), this means that $\frac{\Delta V}{V} = 0$ when the far field load $\boldsymbol{\varepsilon}^{\infty}$ is simple shear. In other words, the volume of the liquid inclusion does not change under simple shear. Because any load can be superposed by combining uni-axial loadings and simple shear, we only need to focus on the uni-axial load for the investigation of the inclusion volume response.

2. Uniaxial stressing affects volumetric behavior of the inclusion differently depending upon the direction of loading.

We then considered uniaxial far-field loading in the direction of one of the major axes of the elliptical inclusions, so that $\boldsymbol{\varepsilon}^{\infty} = \varepsilon(1 + \nu)\left(\boldsymbol{e}_i \otimes \boldsymbol{e}_i\right) - \nu\varepsilon\boldsymbol{I}$, where $\boldsymbol{e}_i$ is a unit vector in the direction of one of the three Cartesian axes, and hence one of the directions of the axes of the ellipse. $\varepsilon > 0$ represents stretching and $\varepsilon < 0$ represents compression.

To model the observation that cells and ECM tend to match their effective mechanical properties, we focused on the case of

$$\frac{k}{K_m} = 1, \tag{11}$$

where $K_m = E/[3(1 - 2\nu)]$ is the bulk modulus of the matrix. Thus, the effective bulk moduli of both the cell and ECM are identical, but the two are fundamentally different because the cell is a kind of fluid compared to the ECM.

The fact that the cell is a fluid led to a radically different mechanical response, which depends on the aspect ratios a_2/a_1 and a_3/a_1 of the ellipsoid (Fig. 2). We set $\nu = 0.3$ in these cases. By comparing the dilatation of the ellipsoid to that of the equivalent bulk ECM, we observed that loading along the two shorter axes causes the greatest volume change, while loading along the longest axis causes the least volume change. For loading along both the longest and intermediate axes, the response is only a very weak function of the aspect ratio a_2/a_1, but a much stronger function of the aspect ratio a_3/a_1, indicating that the smallest dimension dominates the response. Therefore, the thinner the ellipsoid is, the greater the response is. For loading along the thinnest direction, the dependence on aspect ratio is nonlinear and monotonic.

For cases of spheroidal inclusions ($a_1 \approx a_2$ or $a_2 \approx a_3$), which are common in biology and geology [29], we

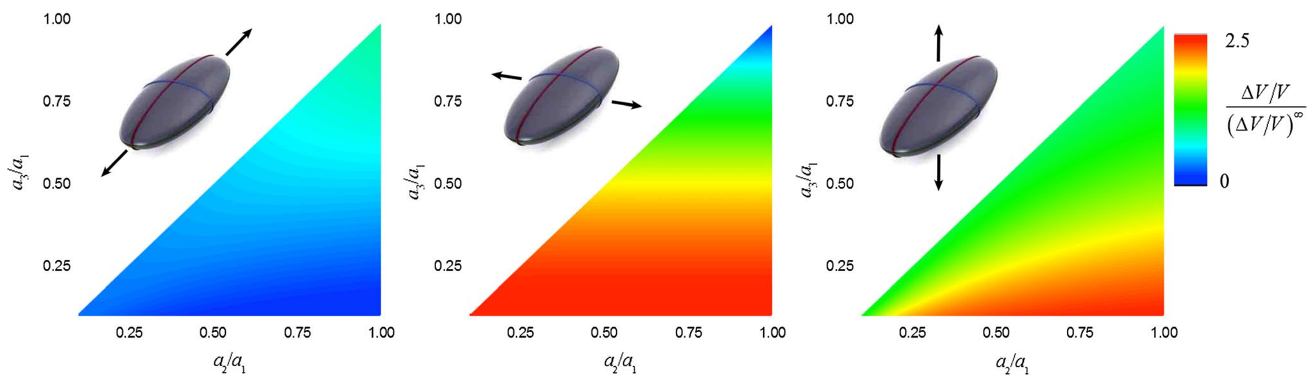

Fig. 2 Volumetric responses of ellipsoidal, compressible liquid inclusions within matrices that are stretched along each of the cell axes. For all panels, $3k(1-2\nu)/E = 1$ and $\nu = 0.3$

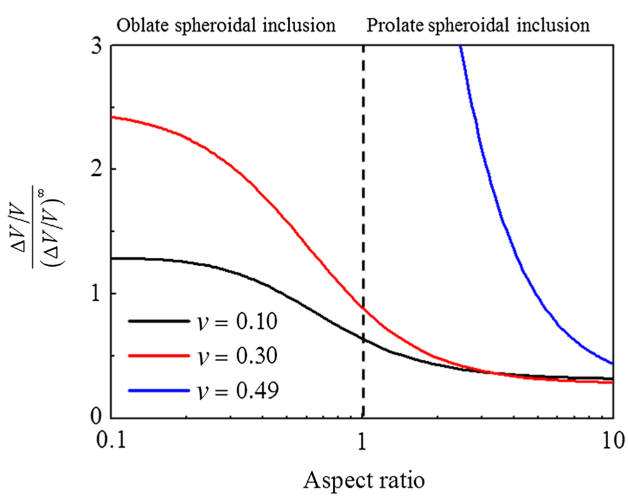

Fig. 3 Volumetric response of spheroidal inclusions. For prolate spheroidal inclusions ($a_1 \geq a_2 = a_3$), the aspect ratio is defined as a_1/a_2. For oblate spheroidal inclusions ($a_1 = a_2 \geq a_3$), the aspect ratio is defined as a_2/a_3. The dashed line is the boundary line between prolate spheroidal inclusions and oblate spheroidal inclusions. Solid lines with different colors represent different Poisson ratios of the matrix. Here, $3k(1-2\nu)/E = 1$

observed that dilatation decreases with increasing aspect ratio with load along the axis of symmetry (Fig. 3). A very strong effect on Poisson ratio of the matrix is evident for oblate spheroids. For prolate spheroids, there is an asymptotic behavior that is independent of Poisson's ratio.

4 Discussion

Loading direction causes tremendously different volume responses for ellipsoidal inclusions. What does this mean for cell alignment in a loaded 3D matrix? Several groups found that cells rearrange along the direction of uni-axial load [30–32]. Explanations for this, as described in the introduction, include certain aspects of stress fiber kinetics and stress limits on stress fibers. However, the results presented here suggest an alternative hypothesis. Given that sufficient loading, and even moderate cyclical loading, can lead to the fluidization of cell cytoskeletons, and given that such loading is implicated in cell rearrangements and realignments, it is reasonable to explore the possibility that volumetric changes are important in cell realignment. This paper contributes two relevant results that provide insight. The first is that, for the small perturbations of linear elasticity, shear and normal strains decouple in volumetric responses of cells, with only normal straining contributing to dilatation. The second is that, with the exception of cells that are nearly spherical, uniaxial load leads to dramatically enhanced dilatation for loadings that are not parallel to the long axis of a cell. The upshot of this observation is that cell rearrangement might arise from a minimization of volume change along the direction of loading.

An additional result of interest is the very strong effect of Poisson's ratio for oblate inclusions. Because Poisson's ratio can be tuned by the regulation of molecules such as proteoglycans in a cell's local microenvironment, this offers a tool by which cells can tune their volumetric responses through molecular synthesis. Taken together, these observations suggest a new bio-physical view to understanding cell alignment in a 3D matrix.

5 Conclusion

We investigated the volumetric response of an ellipsoidal liquid inclusion embedded in a strained 3D matrix. Our analytical expression for this reveals that loading along the shortest axis can cause the greatest volume change, while loading along the longest axis can cause the least volume change. We also find a strong role of Poisson's ratio. We hypothesize that these effects may play a significant role in the development of cell shape and polarity.

Acknowledgements This work was supported by the National Natural Science Foundation of China (Grants 11522219 and 11532009), the National Institutes of Health (Grant U01EB016422), and the National Science Foundation through the Science and Technology Center for Engineering Mechanobiology (Grant CMMI 1548571).

References

1. Giordano, S., Colombo, L.: Effects of the orientational distribution of cracks in solids. Phys. Rev. Lett. **98**(5), 055503 (2007)
2. Bartlett, M.D., Fassler, A., Kazem, N., et al.: Stretchable, high-k dielectric elastomers through liquid-metal inclusions. Adv. Mater. **28**(19), 3726–3731 (2016)
3. Owuor, P.S., Hiremath, S., Chipara, A.C., et al.: Nature inspired strategy to enhance mechanical properties via liquid reinforcement. Adv. Mater. Interfaces **4**(16), 1700240 (2017)
4. Miriyev, A., Stack, K., Lipson, H.: Soft material for soft actuators. Nat. Commun. **8**(1), 596 (2017)
5. Cairns, D.R., Genin, G.M., Wagoner, A.J., et al.: Amplified stain-rate dependence of deformation in polymer-dispersed liquid-crystal materials. Appl. Phys. Lett. **75**(13), 1872–1874 (1999)
6. Elson, E.L., Genin, G.M.: The role of mechanics in actin stress fiber kinetics. Exp. Cell Res. **319**(16), 2490–2500 (2013)
7. Guo, M., Pegoraro, A.F., Mao, A., et al.: Cell volume change through water efflux impacts cell stiffness and stem cell fate. Proc. Natl. Acad. Sci. USA **114**(41), 201705179 (2017)
8. Chen, C., Krishnan, R., Zhou, E.H., et al.: Fluidization and resolidification of the human bladder smooth muscle cell in response to transient stretch. PLoS ONE **5**(8), e12035 (2010)
9. Krishnan, R., Park, C.Y., Lin, Y.C., et al.: Reinforcement versus fluidization in cytoskeletal mechanoresponsiveness. PLoS ONE **4**(5), e5486 (2009)
10. Lee, S.L., Nekouzadeh, A., Butler, B., et al.: Physically-induced cytoskeleton remodeling of cells in three-dimensional culture. PLoS ONE **7**(12), e45512 (2012)
11. De, R., Safran, S.A.: Dynamical theory of active cellular response to external stress. Phys. Rev. E Stat. Nonlinear Soft Matter Phys. **78**, 031923 (2008)
12. De, R., Zemel, A., Safran, S.A.: Dynamics of cell orientation. Nat. Phys. **3**(9), 655–659 (2007)
13. Mcgarry, J.P., Fu, J., Yang, M.T., et al.: Simulation of the contractile response of cells on an array of micro-posts. Philos. Trans. R. Soc. Lond. Math. Phys. Eng. Sci. **2009**(367), 3477–3497 (1902)
14. Hsu, H.J., Lee, C.F., Kaunas, R.: A dynamic stochastic model of frequency-dependent stress fiber alignment induced by cyclic stretch. PLoS ONE **4**(3), e4853 (2009)
15. Kaunas, R., Hsu, H.J.: A kinematic model of stretch-induced stress fiber turnover and reorientation. J. Theor. Biol. **257**(2), 320–330 (2009)
16. Li, Y., Huang, G.Y., Li, M.X., et al.: An approach to quantifying 3D responses of cells to extreme strain. Sci. Rep. **6**, 19550 (2016)
17. Babaei, B., Davarian, A., Lee, S.L., et al.: Remodeling by fibroblasts alters the rate-dependent mechanical properties of collagen. Acta Biomater. **37**, 28–37 (2016)
18. Marquez, J.P., Genin, G.M.: Whole cell mechanics of contractile fibroblasts: relations between effective cellular and extracellular matrix moduli. Philos. Trans. **2010**(368), 635–654 (1912)
19. Marquez, J.P., Genin, G.M., Zahalak, G.I., et al.: The relationship between cell and tissue strain in three-dimensional bio-artificial tissues. Biophys. J. **88**(2), 778–789 (2005)
20. Ducloué, L., Pitois, O., Goyon, J., et al.: Coupling of elasticity to capillarity in soft aerated materials. Soft Matter **10**(28), 5093–5098 (2014)
21. Mora, S., Pomeau, Y.: Softening of edges of solids by surface tension. J. Phys. Condens. Matter Inst. Phys. J. **27**(19), 194112 (2015)
22. Wang, Y., Henann, D.L.: Finite-element modeling of soft solids with liquid inclusions. Extreme Mech. Lett. **9**, 147–157 (2016)
23. Eshelby, J.D.: The determination of the elastic field of an ellipsoidal inclusion, and related problems. Proc. R. Soc. Lond. A Math. Phys. Eng. Sci. **241**(1226), 376–396 (1957)
24. Shafiro, B., Kachanov, M.: Materials with fluid-filled pores of various shapes: effective elastic properties and fluid pressure polarization. Int. J. Solids Struct. **34**(27), 3517–3540 (1997)
25. Chen, X., Li, M.X., Yang, M., et al.: The elastic fields of a compressible liquid inclusion. Extreme Mech. Lett. **22**, 122–130 (2018)
26. Mancarella, F., Style, R.W., Wettlaufer, J.S.: Interfacial tension and a three-phase generalized self-consistent theory of non-dilute soft composite solids. Soft Matter **12**(10), 2744–2750 (2016)
27. Style, R.W., Wettlaufer, J.S., Dufresne, E.R.: Surface tension and the mechanics of liquid inclusions in compliant solids. Soft Matter **11**(4), 672–679 (2015)
28. Eshelby, J.: The elastic field outside an ellipsoidal inclusion. Proc. R. Soc. Lond. A Math. Phys. Eng. Sci. **252**(1271), 561–569 (1959)
29. David, E.C., Zimmerman, R.W.: Compressibility and shear compliance of spheroidal pores: exact derivation via the Eshelby tensor, and asymptotic expressions in limiting cases. Int. J. Solids Struct. **48**(5), 680–686 (2011)
30. Gauvin, R., Parenteau-Bareil, R., Larouche, D., et al.: Dynamic mechanical stimulations induce anisotropy and improve the tensile properties of engineered tissues produced without exogenous scaffolding. Acta Biomater. **7**(9), 3294–3301 (2011)
31. Grenier, G., Remy-Zolghadri, M., Larouche, D., et al.: Tissue reorganization in response to mechanical load increases functionality. Tissue Eng. **11**(2), 90–100 (2005)
32. Kanda, K., Matsuda, T.: Mechanical stress-induced orientation and ultrastructural change of smooth muscle cells cultured in three-dimensional collagen lattices. Cell Transpl. **3**(6), 481–492 (1994)